Papers

Seasonal variability in the optical properties of Baltic aerosols

Agnieszka Zdun[1,*]
Anna Rozwadowska[1]
Susanne Kratzer[2]

[1] Institute of Oceanology,
Polish Academy of Sciences,
Powstańców Warszawy 55, PL–81–712 Sopot, Poland;

e-mail: zdun@iopan.gda.pl

*corresponding author

[2] Stockholm University,
Svante Arrheniusvägen 21A, SE–106 91 Stockholm, Sweden

Abstract

A five-year dataset of spectral aerosol optical thickness was used to analyse the seasonal variability of aerosol optical properties (the aerosol optical thickness (AOT) at wavelength $\lambda = 500$ nm, AOT(500) and the Ångström exponent for the 440–870 nm spectral range, $\alpha(440, 870)$) over the Baltic Sea and dependence of these optical properties on meteorological factors (wind direction, wind speed and relative humidity). The data from the Gotland station of the global radiometric network AERONET (Aerosol Robotic Network, http://aeronet.gsfc.nasa.gov) were taken to be representative of the Baltic Sea conditions. Meteorological observations from Fårosund were also analysed.

Analysis of the data from 1999 to 2003 revealed a strong seasonal cycle in AOT(500) and $\alpha(440, 870)$. Two maxima of monthly mean values of AOT(500) over the Baltic were observed. In April, an increase in the monthly mean aerosol optical thickness over Gotland most probably resulted from agricultural waste straw

The complete text of the paper is available at http://www.iopan.gda.pl/oceanologia/

burning, mainly in northern Europe and Russia as well as in the Baltic states, Ukraine and Belarus. During July and August, the aerosol optical thickness was affected by uncontrolled fires (biomass burning). There was a local minimum of AOT(500) in June.

Wind direction, a local meteorological parameter strongly related to air mass advection, is the main meteorological factor influencing the variability of aerosol optical properties in each season. The highest mean values of AOT(500) and $\alpha(440, 870)$ occurred with easterly winds in both spring and summer, but with southerly winds in autumn.

1. Introduction

Atmospheric aerosols are an important component of the atmosphere. Through their direct (extinction) and indirect (modification of cloud microstructure) interaction with solar radiation and the Earth's thermal radiation, they affect the radiative balance of the atmosphere and stimulate climate variability (d'Almeida et al. 1991, Pan et al. 1997, Seinfeld & Pandis 1998, Kauffman et al. 2001, Chylek et al. 2003, Stigebrandt & Gustafsson 2003, Satheesh & Moorthy 2005). Aerosols are also a crucial problem in the atmospheric correction of remote sensing measurements. In order to validate satellite data, one needs to measure optical properties when satellites pass over the area of investigation (Gao et al. 2000, Ruddick et al. 2000, Holton et al. 2003, Ichoku et al. 2004, Schroeder et al. 2007, Kratzer & Vinterhav 2010).

The content of aerosols in an atmospheric column and the aerosol optical properties depend on the physical parameters of the atmosphere: air humidity and pressure, wind speed and direction. The wind speed is an important factor influencing the generation and transport of aerosols in the atmosphere (Kastendeuch & Najjar 2003, Smirnov et al. 2003, Glantz et al. 2006). The optical properties of aerosols also depend on the history of advecting air masses. Wind direction can be treated as a substitute for an air trajectory (Reiff et al. 1986, Smirnov et al. 1994, Birmilli et al. 2001, Formenti et al. 2001, Pugatshova et al. 2007).

Some aerosol particles, such as ammonium sulphate $(NH_4)_2SO_4$, sea salt and ammonium nitrate NH_4NO_3 are hygroscopic. Changes in relative humidity modify their size distribution and refractive index and hence the optical properties of the aerosol, including the scattering coefficient (Tang 1996, Swietlicki et al. 1999, Terpugowa et al. 2004, Kuśmierczyk-Michulec 2009). Jeong et al. (2007) demonstrated an exponential dependence of the aerosol optical thickness on relative humidity. A strong correlation of spectral aerosol optical thickness with precipitable water, especially for continental air masses, was shown by Rapti (2005). A weaker dependence was observed for air masses of maritime origin.

The aim of this work was to analyse the seasonal changes in the optical properties of Baltic aerosols as well as the dependence of these properties on meteorological conditions, i.e. humidity, and wind speed and direction.

The analysis is based on aerosol optical thickness (AOT) spectra obtained from the AERONET (Aerosol Robotic Network) station on Gotland (57°55′N, 18°57′E), which was selected as being representative of the Baltic Sea area (Holben et al. (1998), web site: http://aeronet.gsfc.nasa. gov). The following parameters were analysed: the aerosol optical thickness for $\lambda = 500$ nm (AOT(500)) and the Ångström exponent computed for the spectral range $\lambda = 440$–870 nm ($\alpha(440, 870)$).

Numerous studies have dealt with aerosol optical properties, e.g. Dubovik et al. (2002) and Eck et al. (1999). However, only in a few has the influence of meteorological parameters on the optical properties of aerosols in the Baltic area been analysed (Smirnov et al. 1995, Kuśmierczyk-Michulec & Rozwadowska 1999, Kuśmierczyk-Michulec & Marks 2000, Kuśmierczyk-Michulec et al. 2001, Kuśmierczyk-Michulec et al. 2002).

In the papers by Kuśmierczyk-Michulec et al. (2001) and Kuśmierczyk-Michulec et al. (2002) the changes in the optical properties of aerosols were analysed as a function of their chemical composition. On the basis of data gathered during two Baltic cruises (July 1997 and March 1998), those authors showed that the maritime aerosols were characterized by the lowest values of the Ångström exponent ($\alpha(400, 865) \leq 0.26$). The presence of organic carbon, mineral aerosols and ammonium salts caused a significant increase in the Ångström exponent. Values of $\alpha(400, 865)$ were the highest when aerosols were dominated by soot particles ($\alpha(400, 865) \geq 1.47$).

Kuśmierczyk-Michulec & Rozwadowska (1999) analysed the seasonal variability in the optical proprieties of Baltic aerosols as well as the influence of meteorological factors on AOT(555) and $\alpha(412, 875)$, taking the northerly (270°–N–90°) and southerly (90°–N–270°) wind sectors into account on the basis of the dataset collected over a four-year period from 1994 to 1998. They found that higher values of the aerosol optical thickness (AOT(555)) and Ångström exponent ($\alpha(412, 875)$) occurred during southerly winds almost regardless of season. Higher values of $\alpha(412, 875)$ occurred only during the summer when winds were northerly. That analysis also showed that with increasing relative humidity RH, there was a greater probability of AOT(555) values being higher.

Niemi et al. (2003, 2005) studied cases of air advection from Europe and eastern Russia above the Scandinavian Peninsula in spring and summer 2002. Focusing on chemical analyses, they found that the aerosols had been generated by forest fires in the above-mentioned areas.

The aerosol optical thickness spectra from 1999 to 2002 from the AERONET station on Gotland were investigated by Carlund et al. (2005). Those authors found only a weak correlation of AOT(500) and $\alpha(440, 870)$ with water vapour and relative humidity. Their analysis did not reveal any significant influence of wind direction and speed on $\alpha(440, 870)$.

Most data used in the papers on the Baltic aerosols have come from short-term campaigns. Only Carlund et al. (2005) analysed AERONET data from Gotland, but they did not take the seasonal changes in aerosol optical properties into consideration. That is why the seasonal variability of aerosol properties over the Baltic Sea as well as the influence of local meteorological factors on the aerosol optical thickness and Ångström exponent are analysed in the present paper.

The paper is organized as follows. Section 2 describes the database and the methods used in the analysis, the results and their discussion are presented in section 3, and section 4 contains conclusions.

2. Material and methods

The basic dataset used in this work – spectra of the aerosol optical thickness AOT(λ) – comes from the AERONET (Aerosol Robotic Network) station on Gotland. The station is equipped with a Cimel Electronique 318 A spectral radiometer. The methods used to measure solar radiation and the instrument description are given, e.g. in Holben et al. (1998) or Smirnov et al. (2003). Only the data for clear sky situations (level 2.0) are employed in this study, i.e. the data following automatic cloud-screening and visual correction by the operator. The algorithms for cloud-screening and the retrieval of aerosol properties are given in Dubovik & King (2000) and Smirnov et al. (2000). The measurement error of the aerosol optical thickness is estimated to be in the range of 0.01–0.02 for $\lambda > 380$ nm, and 0.02 for UV (Holben et al. 1998, Eck et al. 1999).

The Gotland AERONET station (57°55′N, 18°57′E) lies in the northern part of the island of Gotland, 50 m inshore (Figure 1). Owing to the location of the island in the central Baltic Sea this station was adopted as being representative of Baltic Sea conditions. The data collected at the Gotland station from 1999 to 2003 comprise about 11 200 measurements, which are distributed unevenly over the measurement period. Because of the small amount of data available in winter, the winter periods were not taken into consideration in this study.

A meteorological dataset from the Fårosund meteorological station (57°55′N, 18°58′E) from 1999–2003 was also used in the present paper. In particular, observations of wind speed and direction and relative humidity
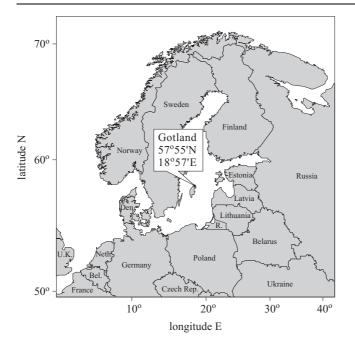
Figure 1. The Baltic Sea basin and the site of the AERONET station (57°55′N 18°57′E) on the island of Gotland

were used. The station is located near the Gotland AERONET station. Meteorological observations were registered every 3 hours.

The wavelength dependence of aerosol optical thickness can be expressed using an empirical formula described by Ångström (Weller & Leiterer 1988, Smirnov et al. 1994, Eck et al. 1999, Carlund et al. 2005):

$$\text{AOT} = \beta\lambda^{-\alpha}. \tag{1}$$

The coefficient β characterizes the degree of atmospheric turbidity due to aerosols and equals the aerosol optical thickness for $\lambda = 1\ \mu\text{m}$. The exponent $\alpha(\lambda_1, \lambda_2)$ (Ångström exponent) determines the slope of spectral AOT(λ) on a log-log scale (Smirnov et al. 1994), and for the spectral range from λ_1 to λ_2 it can be expressed as follows:

$$\alpha(\lambda_1,\ \lambda_2) = \frac{\ln \text{AOT}(\lambda_1) - \ln \text{AOT}(\lambda_2)}{\ln \lambda_1 - \ln \lambda_2}; \tag{2}$$

$\alpha(\lambda_1, \lambda_2)$ as defined in formula (2) is sensitive to errors in AOT(λ) measurements, which are rather high when the aerosol content in the atmosphere is low. To minimize this error individual spectra AOT(λ) were

smoothed by fitting a second order polynomial to the original data (Eck et al. 1999, O'Neill et al. 2001):

$$\ln(\mathrm{AOT}) = a_0 + a_1 \ln \lambda + a_2 (\ln \lambda)^2. \tag{3}$$

The Ångström exponent for the wavelength range $\lambda = 440$–870 nm was calculated on the basis of formula (2). The data were additionally examined with respect to their quality. We could not test data quality on the basis of sky observations because cloud observations were not made at either
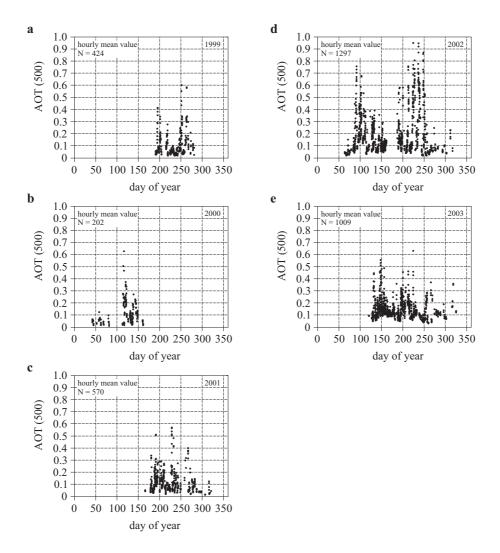

Figure 2. Seasonal distribution of AOT(500) for: a) 1999 (9 July to 7 October), b) 2000 (11 February to 9 June), c) 2001 (15 June to 16 November), d) 2002 (5 March to 12 November), e) 2003 (28 April to 20 November)

the Gotland AERONET station or the Fårosund meteorological station. Instead, we analysed the daily trend of AOT(500) and $\alpha(440, 870)$. The divergence of AOT(500) and $\alpha(440, 870)$ from the respective daily trends suggested the presence of thin clouds. Such measurements were rejected. The next step in the analysis was the calculation of the hourly mean values of both parameters, i.e. AOT(500) and $\alpha(440, 870)$. Further in this paper, the hourly means are treated as individual measurements and are denoted as AOT(500) and $\alpha(440, 870)$ without an averaging sign. As mentioned before, the data were not evenly distributed in time. Figure 2 illustrates the temporal distribution of hourly mean values of AOT(500), and Table 1 lists the number of hourly means in the individual months.

Table 1. Number of hourly means of AOT(500) and $\alpha(440, 870)$ in every measuring month of the Gotland AERONET station dataset

Month Year	Feb.	March	April	May	June	July	August	Sept.	Oct.	Nov.	Sum
1999						109	157	150	8*		424
2000	26*	19*	55	91	11*						202
2001					33	251	165	59	46	16*	570
2002		120	209	228	131	185	235	145	35	9*	1297
2003			6*	209	234	217	150	139	41	13*	1009
Data	26	139	270	528	409	762	707	493	130	38	3502

*not analysed

   Summer months have the largest number of data (N = 762 in July and N = 707 in August). The least data are available for February (N = 26) and November (N = 38). Therefore, data relating to late autumn and winter were rejected from the analysis. Months not taken into consideration in the further analysis are marked with an asterisk in Table 1. The whole dataset was divided into three seasons: spring (March, April, May), summer (June, July, August) and autumn (September, October). The data from each season were analysed separately.

   The phrases 'five-year monthly mean of the aerosol optical thickness' and 'five-year monthly mean of the Ångström exponent' used in the present work denote the respective mean values calculated from all measurements available for a given month from the period 1999–2003. Means were marked as $< AOT(500) >$ and $< \alpha(440, 870) >$ with indices 'sp', 'su' and 'a' for spring, summer, and autumn, as well as N (North), E (East), S (South), W (West) for wind directions and III–X for the respective months. It should be noted that only the measurements from 2002 covered all the seasons; the coverage in the other years relates only to certain parts of the year.

Furthermore, trajectories of air advected over Gotland were used to interpret the temporal (intra- and interannual) variability of the optical properties of Baltic aerosols. Six-day backward trajectories of air advected to the Gotland station at heights of $h = 300$ m, $h = 500$ m and $h = 3000$ m above sea level were calculated by the HYSPLIT model (version 4) (Draxler & Rolph 2003, Rolph 2003). Additional information on types of air mass was obtained from twenty-four hour synoptic maps from the period 2001 –2003, available from the Institute of Meteorology and Water Management (IMGW) in Gdynia, Poland.

3. Results and discussion

3.1. Seasonal variability in aerosol optical thickness and Ångström exponent

In order to examine the variability in the optical properties of Baltic aerosols (i.e. the aerosol optical thickness for $\lambda = 500$ nm and the Ångström exponent in the $\lambda = 440$–870 nm range) the measurement year was divided into three seasons: spring (March, April, May), summer (June, July, August) and autumn (September, October). The respective numbers of data (N in Table 2) in each season were 890, 1865 and 611.

The frequency distributions of the hourly mean values of AOT(500) and $\alpha(440, 870)$ for each season are shown in Figure 3. The respective interval widths are 0.025 and 0.125 in the case of the frequency distributions of the aerosol optical thickness and the Ångström exponent. Histograms of AOT(500) vary from a sharp distribution (Figure 3c) with a modal value of 0.050 for autumn to broader distributions with a modal value of 0.075 for the spring and summer seasons (Figures 3a, 3b). The distributions are skewed towards higher values (right-skewed).

All histograms of $\alpha(440, 870)$ are skewed towards lower values (left-skewed) (Figures 3d–3f). The most probable respective values for spring, summer and autumn seasons are 1.375, 1.750 and 1.625. The distribution of $\alpha(440, 870)$ for summer is sharper than during spring and autumn conditions.

Many papers relate aerosol optical properties, e.g. the Ångström exponent, to a type of aerosol. However, the threshold for $\alpha(440, 870)$ usually used to distinguish marine aerosols varies depending on the author. Kuśmierczyk-Michulec et al. (2001) and Kuśmierczyk-Michulec et al. (2002) adopted a threshold of 0.26 (i.e. $\alpha(400, 865) \leq 0.26$) for those instances when sea salt controls aerosol optical thickness, whereas Smirnov et al. (2003) applied a much higher value of the Ångström exponent ($\alpha(440, 870) \leq 1.0$) and AOT(500) ≤ 0.15 to describe pure marine aerosols.

Table 2. The mean values of the aerosol optical thickness $< AOT(500) >$, Ångström exponent $< \alpha(440, 870) >$ and standard deviation (σ) of Baltic aerosols from 1999–2003 for spring, summer and autumn. $AOT(500)_{mod}$ and $\alpha(440, 870)_{mod}$ are the modal values of the frequency distributions of the aerosol optical parameters for bin sizes 0.025 and 0.125 for $AOT(500)$ and $\alpha(440, 870)$ respectively. 'N' denotes the number of data in each season

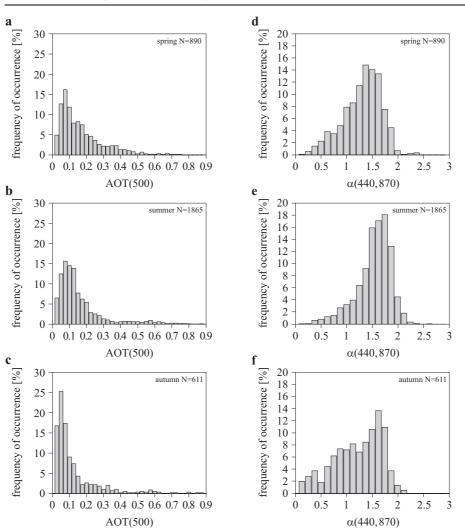| Season	N	AOT(500)		$\alpha(440, 870)$	
		$< AOT(500) > \pm\sigma$	$AOT(500)_{mod}$	$< \alpha(440, 870) > \pm\sigma$	$\alpha(440, 870)_{mod}$
spring	890	0.166 ± 0.126	0.075	1.305 ± 0.374	1.375
summer	1865	0.154 ± 0.136	0.075	1.539 ± 0.341	1.750
autumn	611	0.121 ± 0.133	0.050	1.220 ± 0.466	1.625

Figure 3. Seasonal frequency distributions of the aerosol optical thickness for $\lambda = 500$ nm (a–c) and the Ångström exponent for $\lambda = 440$–870 nm (d–f)

Kuśmierczyk-Michulec (2009) concluded that an Ångström exponent < 0.5 indicates the marine aerosol type, values of $\alpha(440, 870)$ between 1.0 and 1.5 represent the continental aerosol type, and values > 1.5 the industrial aerosol type. Over Gotland, $\alpha(440, 870) \leq 1.0$ only make up 20%, 8% and 32% of observations in spring, summer and autumn respectively. In autumn, Ångström exponents < 1 are more frequently observed (32%) than in the other seasons, which indicates a higher contribution of marine aerosols. Even though the thresholds given above are approximate, the seasonal frequency distributions of the Ångström exponent with modal

values ranging from 1.375 to 1.750 (Figure 3) clearly indicate the high contribution of the mixed continental-industrial type of aerosols in the Baltic atmosphere throughout the year, but especially in summer. On the basis of the same Gotland AERONET station dataset from the period 1999 –2001, Carlund et al. (2005) concluded that normally, the atmosphere over Gotland could be considered clear, with a daily median value of AOT(500) of about 0.08. The median value of $\alpha(440, 870)$ was 1.37, indicating that the dominant aerosol was more of a continental than of a pure marine type.

Means of the seasonal distributions of AOT(500) and $\alpha(440, 870)$ are given in Table 2. The histograms of AOT(500) and $\alpha(440, 870)$ are skewed. Their longer tails contain extreme cases, with AOT(500) several times higher and $\alpha(440, 870)$ several times lower than the respective modal values. The means are sensitive to such atypical extreme cases, and therefore show different values and tendencies than the modal values. The lowest values of $< \mathrm{AOT}(500) >$ and $< \alpha(440,\ 870) >$ (mean $\pm$ standard deviation) were observed during autumn ($< \mathrm{AOT}(500) >_{\mathrm{a}} = 0.121 \pm 0.133$ and $< \alpha(440,\ 870) >_{\mathrm{a}} = 1.220 \pm 0.466$). The highest mean AOT(500) value of 0.166 ± 0.126 was found during spring. The mean of the Ångström exponent reaches its maximum in summer ($< \alpha(440,\ 870) >_{\mathrm{su}} = 1.539 \pm 0.341$). The differences between seasonal means of AOT(500) are statistically significant at the 0.01 level (two-sample unpooled t-test for means, unequal variances).

The mean values of AOT(500) for summer ($< \mathrm{AOT}(500) >_{\mathrm{su}} = 0.154 \pm 0.136$) and autumn ($< \mathrm{AOT}(500) >_{\mathrm{a}} = 0.121 \pm 0.133$) obtained from the present analysis (Table 2) are lower than those given by Kuśmierczyk-Michulec & Rozwadowska (1999) for summer ($\mathrm{AOT}(550) = 0.225 \pm 0.113$) and autumn ($\mathrm{AOT}(550) = 0.225 \pm 0.138$) for the southern Baltic. In spring the reverse situation prevails: $< \mathrm{AOT}(500) >_{\mathrm{sp}} = 0.166 \pm 0.126$ obtained in the current work is higher than the value ($\mathrm{AOT}(550) = 0.155 \pm 0.107$) from Kuśmierczyk-Michulec & Rozwadowska (1999). The differences between the mean AOT(500) obtained from the current analysis and the mean values of aerosol optical thickness measured by Kuśmierczyk-Michulec & Rozwadowska (1999) are statistically significant for summer and autumn, but insignificant for spring at a significance level 0.01 (two-sample unpooled t-test for means, unequal variances). The significant differences may have resulted from differences in time period and area of investigation. Gotland is located north of the Polish economic zone, where most of the measurements by Kuśmierczyk-Michulec & Rozwadowska were made. Moreover, the impact of air flowing in from central and eastern Europe on aerosol optical thickness was much stronger above the southern Baltic than over Gotland.

Clean air masses from the north and the Scandinavian Peninsula were dominant above Gotland in summer and autumn.

The monthly mean aerosol optical thicknesses for $\lambda = 500$ nm from all the available data (1999–2003) are given in Figure 4 (black, thick line in Figure 4). The monthly means of AOT(500) show a bimodal distribution with peaks in April and August. $< \text{AOT}(500) >$ varies from 0.084 ± 0.034 in October to 0.180 ± 0.185 in August and 0.223 ± 0.152 in April. For June,
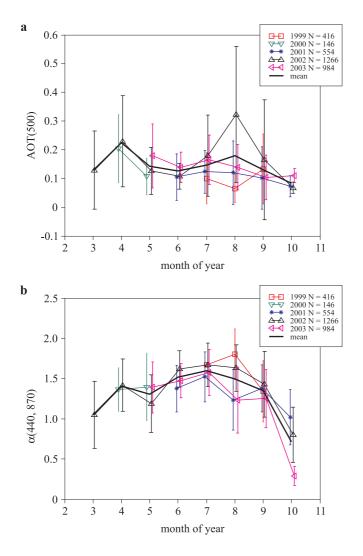

Figure 4. Seasonal changes of monthly means of aerosol optical thickness for $\lambda = 500$ nm (a) and Ångström exponent for $\lambda = 440$–870 nm (b). For clarity, the curves for individual years have been shifted horizontally with respect to each other. Vertical lines denote standard deviations from the mean

a local minimum is observed ($< \mathrm{AOT}(500) >_{\mathrm{VI}} = 0.126 \pm 0.056$). While the April maximum and June and October minimum are also found in the AOT(500) data in individual years contributing to the five-year monthly means, an August maximum occurs only in 2002.

The five-year monthly mean value of the Ångström exponent calculated for all the data available varied from 0.711 ± 0.426 in October to 1.596 ± 0.294 in July. A local maximum of $\alpha(440, 870)$ occurred in April ($< \alpha(440, 870) >_{\mathrm{IV}} = 1.406 \pm 0.314$) and July ($< \alpha(440, 870) >_{\mathrm{VI}} = 1.596 \pm 0.294$), while the minimum ($< \alpha(440, 870) >_{\mathrm{V}} = 1.303 \pm 0.370$) was observed in May.

Compared to the other years within measuring the period 1999–2003, 2002 was conspicuous. The monthly mean values of the aerosol optical thickness in summer 2002 were considerable much than in the other years considered. A particularly high monthly mean AOT(500) for 2002 was recorded in August, when it reached 0.323 ± 0.237. For comparison, the monthly mean aerosol optical thicknesses in the Augusts of the other years varied from 0.065 ± 0.050 in 1999 to 0.139 ± 0.079 in 2003 (Figure 4a). The monthly mean values of $< \alpha(440, 870) >$ from June to September of 2002 also reached exceptionally high values (Figure 4b). The monthly mean values of the aerosol optical thickness AOT(500) in July and August of 1999 were the lowest of all.

The aerosol optical thickness above Gotland is influenced not only by periodic and incidental phenomena near the Baltic Sea shore, but also by distant continental phenomena. The origin of air masses advecting over Gotland has an impact on the aerosol optical thickness as well as the Ångström exponent. Based on a synoptic map analysis of AOT(500) measurements over five years, AOT(500) values < 0.100 were linked to the advection of maritime Arctic and maritime Polar air masses over the Baltic area. The advection of continental Polar air above the Baltic (six-day backward trajectories leading from over central Europe) can increase the aerosol optical thickness up to 0.682 (± 0.025), as observed on 1 April 2002.

In summer 2002, fires intensified by persistent drought contributed to the high values of the aerosol optical thickness. Monthly composite satellite images available from FIRMS (The Fire Information for Resource Management System) show the particularly numerous forest and field fires in northern Europe, Russia, Ukraine and Belarus in 2001 and 2002. Moreover, in summer 2002 the modal wind direction was different from that in the other summers considered here. For example, north-easterly winds ($40°$) were predominant in August 2002, whereas winds from the north-west ($300°$ and $310°$) were the most frequent in 1999, 2001 and 2003. The specific

synoptic situation in 2002 favoured the transport of aerosol towards Gotland derived from the biomass burning. For example, the biomass burning aerosols transported over the Baltic Sea along with advecting air on 31 July or 12 August 2002 resulted in $< \text{AOT}(500) >_{31072002} = 0.661 \pm 0.084$ and $< \text{AOT}(500) >_{12082002} = 0.624 \pm 0.162$. The enlarged emission of aerosol and an increase in AOT(500) in spring was presumably related to agricultural waste straw burning (Niemi 2003).

It is worth noting that during the time period under scrutiny, cases of air advection from Africa at 3000 m above the Baltic region were observed in spring and summer. However, at lower altitudes the air then usually came from the burning regions of Russia, Ukraine and Belarus. In such cases the daily mean aerosol optical thicknesses for $\lambda = 500$ nm were lower (i.e. $< \text{AOT}(500) >_{12042002} = 0.261 \pm 0.055$, $< \text{AOT}(500) >_{12052002} = 0.249 \pm 0.038$, $< \text{AOT}(500) >_{13082002} = 0.416 \pm 0.043$) than AOT(500) measured when the air from above Europe and Asia advected over Gotland at these three altitudes.

The relations between the aerosol optical thickness AOT(500) and the Ångström exponent $\alpha(440, 870)$ for spring, summer and autumn are shown in Figure 5. This visual representation often allows one to define physically interpretable cluster regions for different types of aerosols with different optical properties (El-Metwally et al. 2008). Figure 5 shows that the cases of exceptionally high aerosol load (AOT(500) > 0.500) observed in summer and autumn 2002 are typically associated with a high Ångström exponent (> 1.4). Moreover, $\alpha(440, 870)$ is then almost independent of AOT(500). This rules out the possible impact of thin clouds on aerosol optical thickness in such cases. The Ångström exponent is within the range typical of biomass burning and urban-industrial aerosols (Dubovik et al. 2002), which confirms the advective origin of the aerosol in these cases.

The dependence of aerosol optical properties over the Baltic region on air mass movements was observed by previous researchers. For example, Smirnov et al. (1995) measured aerosol optical thickness AOT(550) of 0.46 and 0.09 and an Ångström exponent of 1.14 and 0.99 for cases of continental Polar and maritime Arctic types of air mass over the Baltic Sea, respectively. For modified maritime Polar air reaching the Baltic region after passing the British Isles and Scandinavia, AOT(550) and $\alpha(460, 1016)$ were respectively equal to 0.45 and 1.37.

3.2. Impact of wind speed and direction on aerosol optical properties

The next step in this work was to examine the influence of wind direction and wind speed on the optical properties of Baltic aerosols, i.e. AOT(500)
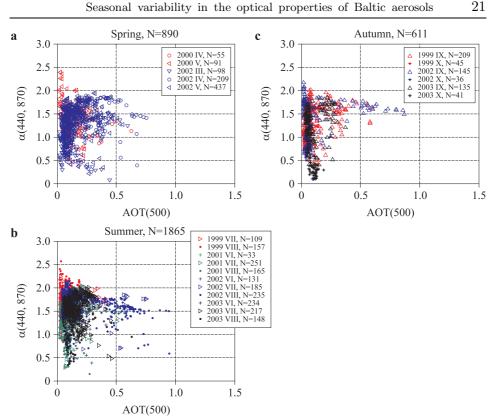
a Spring, N=890

Legend:
- 2000 IV, N=55
- 2000 V, N=91
- 2002 III, N=98
- 2002 IV, N=209
- 2002 V, N=437

y-axis: α(440, 870)
x-axis: AOT(500)

b Summer, N=1865

Legend:
- 1999 VII, N=109
- 1999 VIII, N=157
- 2001 VI, N=33
- 2001 VII, N=251
- 2001 VIII, N=165
- 2002 VI, N=131
- 2002 VII, N=185
- 2002 VIII, N=235
- 2003 VI, N=234
- 2003 VII, N=217
- 2003 VIII, N=148

y-axis: α(440, 870)
x-axis: AOT(500)

c Autumn, N=611

Legend:
- 1999 IX, N=209
- 1999 X, N=45
- 2002 IX, N=145
- 2002 X, N=36
- 2003 IX, N=135
- 2003 X, N=41

y-axis: α(440, 870)
x-axis: AOT(500)

Figure 5. Scatterplot of the Ångström exponent for $\lambda = 440$–870 nm versus the aerosol optical thickness for $\lambda = 500$ nm for a) spring, b) summer and c) autumn

and $\alpha(440, 870)$. For this, we used the wind directions measured at the Fårosund meteorological station.

In order to determine the influence of meteorological factors on the aerosol optical properties the dataset for aerosol optical thickness was divided with respect to wind direction into northerly ($315°$–$45°$), easterly ($45°$–$135°$), southerly ($135°$–$225°$) and westerly ($225°$–$315°$) wind sectors. Aerosol emissions from the surface of the Baltic Sea depend on wind speed. For wind speeds < 6 m s^{-1} an increase in aerosol particle concentration due to increasing wind speed is usually connected with biological and chemical processes occurring at sea. For wind speeds $V_w > 6$ m s^{-1} dynamic processes, such as breaking waves, begin to dominate aerosol generation from the sea surface (Zieliński 2006). There are only a small number of data with high wind speeds in the Gotland dataset from which the crucial generation of seaborne aerosol occurs, i.e. $V_w \geq 10$ m s^{-1} (Petelski 2003). The dataset with $V_w \leq 6$ m s^{-1} constituted 66%, 58% and 55% of all the data in spring,

A. Zdun, A. Rozwadowska, S. Kratzer

Table 3. Aerosol optical parameters from the Gotland AERONET station from 1999 to 2003 for particular wind directions and $V_w \leq 6$ m s^{-1} for spring, summer and autumn. $< \mathrm{AOT}(500) >$ and $< \alpha(440, 870) >$ are the mean values of the respective optical parameter and standard deviation σ. $\mathrm{AOT}(500)_{\mathrm{mod}}$ and $\alpha(440, 870)_{\mathrm{mod}}$ are the modal values of frequency distributions of $\mathrm{AOT}(500)$ and $\alpha(440, 870)$ for bin sizes 0.025 and 0.125 respectively. 'N' denotes the number of data in the northerly (N), easterly (E), southerly (S) and westerly (W) wind sectors

Season	Wind sector	N	AOT(500)			$\alpha(440, 870)$		
			$< \mathrm{AOT}(500) >$	σ	$\mathrm{AOT}(500)_{\mathrm{mod}}$	$< \alpha(440, 870) >$	σ	$\alpha(440, 870)_{\mathrm{mod}}$
spring	315°–N–45°	176	0.176	0.129	0.050	1.385	0.397	1.625
	45°–E–135°	133	0.183	0.126	0.075	1.391	0.345	1.500
	135°–S–225°	149	0.162	0.103	0.100	1.361	0.301	1.375
	225°–W–315°	198	0.168	0.139	0.075	1.306	0.331	1.250
summer	315°–N–45°	586	0.136	0.117	0.100	1.593	0.304	1.875
	45°–E–135°	312	0.240	0.206	0.100	1.615	0.303	1.875
	135°–S–225°	251	0.194	0.134	0.150	1.550	0.303	1.750
	225°–W–315°	306	0.115	0.217	0.050	1.531	0.326	1.625
autumn	315°–N–45°	108	0.103	0.091	0.050	1.245	0.425	1.500
	45°–E–135°	59	0.090	0.078	0.025	1.126	0.342	0.875
	135°–S–225°	109	0.203	0.217	0.050	1.393	0.419	1.625
	225°–W–315°	122	0.111	0.107	0.025	1.337	0.494	1.750

summer and autumn respectively. The number of observations, divided into season and wind direction, is shown in Table 3.

An example of the seasonal dependence of aerosol optical thickness for $\lambda = 500$ nm on wind velocity is shown in Figure 6 for westerly winds in summer. The highest AOT(500) values (cases of advection from the continent) occurred for low wind speeds ($V_w \leq 6$ m s^{-1}), which mask the impact of local marine aerosol generation on AOT(500). AOT(500) for the marine aerosol is much lower than for cases of, say, advective biomass burning. The data presented in Figure 6 have Pearson's correlation coefficient R = 0.08. The AOT(500) values used in the correlation coefficient computations were the means over 1 m s^{-1} bins of wind speed. Only a slight increase in the AOT(500) minimum was found with increasing wind speed. For the other seasons and wind directions, the dependence of wind speed upon aerosol optical thickness is even weaker and R is typically negative. For southerly and easterly winds the impact of the sea is additionally weakened by the passage of the air over the island before reaching the station. Only cases with $V_w \leq 6$ m s^{-1} are used in the subsequent analysis.
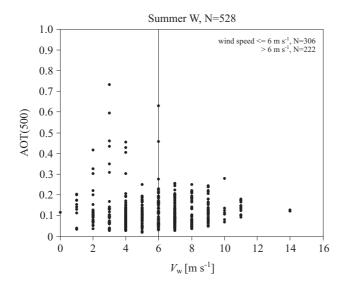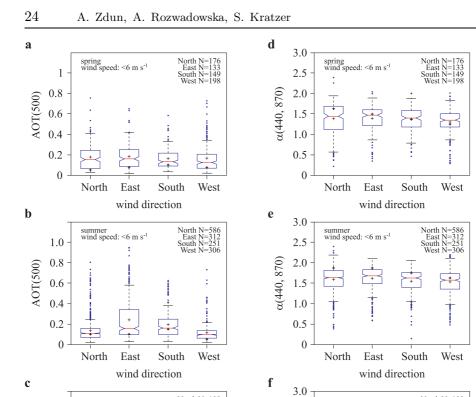

Figure 6. An example of changes in the aerosol optical thickness for $\lambda = 500$ nm versus wind velocity for all data in the westerly wind sector in summer (N = 528)

Figure 7 shows the dependence of AOT(500) and of α(440, 870) on wind direction for each season. The symbol '+' represents the seasonal mean values of AOT(500) and α(440, 870). The symbol '*' shows the

Figure 7. Dependence of AOT(500) and $\alpha(440–870)$ on northerly, southerly, easterly and westerly winds for spring, summer and autumn. '+' – the mean value, symbol '*' – modal value of distribution; the red line denotes the median; the other lines are the 10th, 25th, 75th, 95th percentiles

modal value of the respective distributions. The red line denotes the median value and the remaining lines indicate the 10th, 25th, 75th and 95th percentiles of the respective frequency distribution. The highest mean values of AOT(500) were found for easterly winds in spring and summer (Figures 7a, 7b): they are equal to 0.183 ± 0.126 and 0.240 ± 0.206 respectively. The lowest values of $< \text{AOT}(500) >$ were recorded for southerly winds in spring ($< \text{AOT}(500) >_{\text{sp,S}} = 0.162 \pm 0.103$) and for westerly winds

in summer ($< \text{AOT}(500) >_{\text{su, W}} = 0.115 \pm 0.093$). In autumn $< \text{AOT}(500) >$ varied from 0.090 ± 0.080 to 0.203 ± 0.212 for easterly and southerly winds respectively (Figure 7c). The maximum of the mean Ångström exponent $< \alpha(440, 870) >$ in each season occurred in those wind sectors where the values of $< \text{AOT}(500) >$ were also the highest (Figure 7, Table 3), i.e. for easterly winds in spring and summer ($< \alpha(440, 870) >_{\text{sp, E}} = 1.391 \pm 0.345$ and $< \alpha(440, 870) >_{\text{su, E}} = 1.615 \pm 0.303$) and for southerly winds in autumn ($< \alpha(440, 870 >_{\text{a, S}} = 1.393 \pm 0.419$). The aerosol optical properties for each wind direction and season are given in Table 3.

The mean values of $\text{AOT}(500)$ for a given wind direction can be explained by the occurrence of maritime and continental air advection over Gotland. In the present paper, this analysis is performed only for summer. In spring, the difference between the highest and the lowest $< \text{AOT}(500) >$ for a given wind direction is low. In autumn, too few synoptic maps were available for us to draw any conclusions for that season. Therefore, there are no analyses for spring and autumn in this paper.

In summer, in 43% of 45 cases of easterly winds with the highest $< \text{AOT}(500) >$, 24 h synoptic maps (see section 2) indicated the presence of continental Polar air above Gotland. Clear maritime Polar air accounted for 33% of cases, and Arctic air masses for 22%. Moreover, during 2002 the large number of fires over Europe and Asia made a significant contribution to the easterly wind sector (61%). For westerly winds with the lowest mean value of $\text{AOT}(500)$ the contribution of continental Polar air over Gotland was lower, i.e. 11% out of 38 available 24 h synoptic maps in summer, whereas maritime Polar air was dominant (65%), and the Arctic air contribution accounted for 24%.

The dependence of modal values on the seasonal distributions of $\text{AOT}(500)$ and $\alpha(440, 870)$ on wind direction are more intuitive than the corresponding dependence of the respective mean values. The highest modal values of $\text{AOT}(500)$ distributions, marked in Figure 7 with an asterisk, are found for southerly winds in spring and summer (0.100 and 0.150 respectively), which implies a continental influence on the aerosol optical properties above Gotland. The lowest modal values of $\text{AOT}(500)$ distributions occurred for northerly winds in spring and westerly winds in summer. In autumn, modal values of $\text{AOT}(500)$ varied weakly from 0.025 to 0.050.

The most probable values of the Ångström exponent show different tendencies (Figures 7d–7f). In spring and summer a maximum of $\alpha(440, 870)_{\text{mod}}$ occurred for northerly winds (1.625 and 1.875), and also in summer for easterly winds (1.875). In autumn, the modal values of $\alpha(440, 870)$ changed from 0.875 for easterly winds to 1.875 for westerly

winds. Typically, the distributions of the Ångström exponent are left-skewed in every season. There was one exception for easterly winds in autumn, most probably due to the small number of observations for this case ($N = 59$).

3.3. The impact of relative humidity on aerosol optical properties

Analysing the seasonal influence of humidity on the variability of optical parameters, i.e. AOT(500) and $\alpha(440, 870)$ for different wind directions, the data were also divided into two groups with varying wind speeds, i.e. below and above 6 m s^{-1}. Only the former group is shown here because of the low number of observations and limited range of the relative humidity (RH) in the latter one. In general the relationship between AOT(500) and RH is nonlinear (e.g. Jeong et al. 2007). Two types of correlation coefficient were used to quantify the correlation between mean AOT(500) and RH: Spearman's rank correlation coefficient (RS) and Pearson's linear correlation coefficient (R). Pearson's coefficient was computed for transformed variables

Table 4. Spearman's rank correlation coefficient (RS) and Pearson's linear correlation coefficient (R) for the relationship between the aerosol optical thickness for $\lambda = 500$ nm from the Gotland AERONET station from 1999 to 2003 and the relative humidity (RH) for wind speed $V_w \leq 6$ m s^{-1} for spring, summer and autumn. 'N' denotes the number of data in the northerly (N), easterly (E), southerly (S) and westerly (W) wind sectors

Season	Wind sector	$V_w \leq 6$ m s^{-1}			
		N	RH range [%]	RS	R
spring	315°–N–45°	176	50–90	0.37	−0.34
	45°–E–135°	133	30–90	0.14	−0.09
	135°–S–225°	149	30–90	0.08	−0.07
	225°–W–315°	198	40–90	0.06	−0.08
summer	315°–N–45°	586	40–100	0.55	−0.56
	45°–E–135°	312	30–90	0.05	−0.05
	135°–S–225°	251	40–100	0.07	−0.05
	225°–W–315°	306	30–90	0.19	−0.24
autumn	315°–N–45°	108	50–100	0.40	−0.49
	45°–E–135°	59	50–90	0.66	−0.59
	135°–S–225°	109	50–90	0.15	−0.05
	225°–W–315°	122	40–90	0.22	−0.27

$\ln(\text{AOT}(500))$ and $\ln(100 - \text{RH})$. In accordance with the equation (Jeong et al. 2007)

$$\frac{\sigma_{\text{scat}}(\text{RH})}{\sigma_{\text{scat}}(\text{RH} = 40\%)} = a \left(1 - \frac{\text{RH}(\%)}{100}\right)^{-b}, \tag{4}$$

we assumed the relationship between the transformed variables to be linear (a, b – empirical parameters, $\sigma_{\text{scat}}(\text{RH})$ – aerosol scattering coefficient at a given RH). The coefficients RS and R are given in Table 4. For cases when $V_{\text{w}} \leq 6$ m s^{-1} the most distinct increase in AOT(500) with RH (and the highest absolute value of the correlation coefficient (R)) appeared for northerly winds ($315°$–$45°$) in each season and also for easterly winds in autumn (Table 4, Figures 8a–8c). No correlation was found in the other seasons or wind sectors. The influence of RH on AOT(500) was masked by an increase in AOT(500) at lower humidities because of other factors, e.g. advection or local aerosol generation. It must be noted that the data presented here show aerosol properties occurring at various air humidities rather than the results of the hygroscopic growth of an aerosol of a certain type. In our data set, aerosol load and composition at different humidities may vary. Figure 9 shows examples of AOT(500) versus RH for a case of high correlation (summer, northerly winds, RS = 0.55, Figure 9a) and low correlation (summer, southerly winds, RS = 0.07, Figure 9b).

Variations in the Ångström exponent $\alpha(440, 870)$ with increasing RH were often indiscernible (Figures 8d–8f, 9). An increase in mean $\alpha(440, 870)$ with RH was observed for the N and W wind sectors in spring, the N, E and S sectors in summer and the N and E sectors in autumn. According to the model by Kuśmierczyk-Michulec (2009) an increase in Ångström exponent with growing RH can be found, e.g. for a mixture of sea salt and fine anthropogenic salt NH_4HSO_4 (in the model the effective particle radius was 0.1055 μm).

In comparison, Weller & Leiterer (1998) found that in the Baltic Sea region the impact of RH on the aerosol optical thickness and the Ångström exponent was only noticeable when RH $> 90\%$. Smirnov et al. (1995) were unable to find statistical proof for a correlation between optical parameters and relative humidity for RH $< 80\%$, and neither were Carlund et al. (2005) able to find a correlation between the aerosol optical thickness for $\lambda = 500$ nm and the Ångström exponent with precipitation or relative humidity. The latter study was based on the Gotland AERONET station dataset from the period 1999 to 2002, but the data were not analysed with respect to wind direction or season.
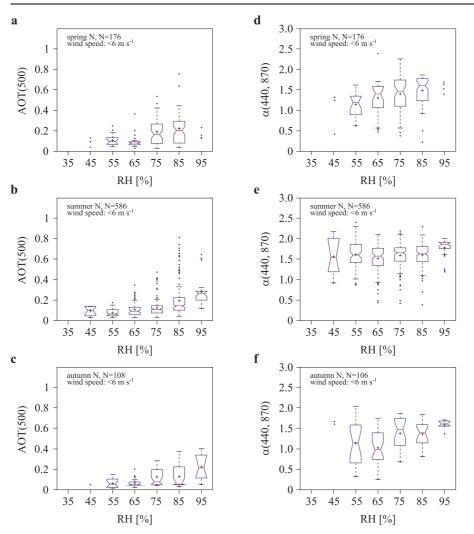
Figure 8. Dependence of the aerosol optical thickness for $\lambda = 500$ nm and the Ångström exponent for $\lambda = 440$–870 nm on relative humidity (RH) for northerly winds in spring, summer and autumn. '+' – the mean value; the red line denotes the median; the other lines are the 10th, 25th, 75th, 95th percentiles

4. Conclusions

- The atmospheric model generated one of the greatest errors we have at the moment for satellite data retrievals over coastal areas as the atmosphere is highly variable. The aerosol composition of the transition zone between land and sea is complex and variable, posing a challenge for the procedures intended to correct the remote sensing signal from the coastal zone for atmospheric influence (Kratzer
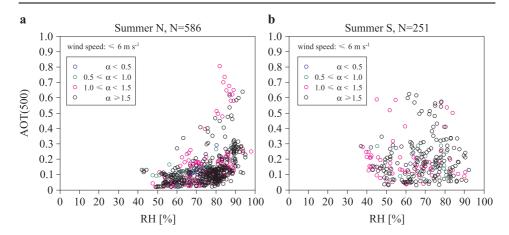
Figure 9. Scatterplot of the aerosol optical thickness for $\lambda = 500$ nm and relative humidity (RH) for wind speeds ≤ 6 m s^{-1} for northerly a) and southerly b) winds in summer. The colours denote the ranges of the Ångström exponent

& Vinterhav 2010). This article shows the aerosol variations clearly, and gives a statistical analysis. The results can be used to validate the atmospheric model above the coastal regions.

- The monthly mean of the aerosol optical thickness at $\lambda = 500$ nm from all available observations from Gotland during 1999–2003 was very variable: it varied from 0.083 ± 0.034 (mean value and standard deviation) in October to 0.180 ± 0.185 in August and 0.223 ± 0.152 in April (Figure 4). For June, a local minimum was observed ($< \text{AOT}(500) >_{VI} = 0.126 \pm 0.056$). The five-year monthly mean of the Ångström exponent calculated for all data available varied from 0.711 ± 0.426 in October to 1.596 ± 0.294 in July. A local maximum of $\alpha(440, 870)$ occurred in April ($< \alpha(440, 870) >_{IV} = 1.406 \pm 0.314$) and July ($< \alpha(440, 870) >_{VII} = 1.596 \pm 0.294$), while a minimum ($< \alpha(440, 870) >_{V} = 1.303 \pm 0.370$) was observed in May. This is connected with the advection of different types of air masses over the Baltic Sea. In summer, the occurrence of forest and field fires in Europe and Russia increased as a result of persistent drought. Aerosol derived from biomass burning was transported over Gotland and contributed to the high values of the aerosol optical thickness. The increased emission of aerosols and the increase in AOT(500) in spring was presumably related to agricultural waste straw burning (Niemi 2003).

- The wind direction seems to have the greatest influence on the variability of aerosol optical properties in every season. The wind

direction is closely connected with the type of air mass and the direction of air advection. The highest mean value of AOT(500) in summer was found during easterly winds (45°–135°) and was equal to 0.240 ± 0.206 (Figure 7b). Here, the contribution of continental air masses was larger than for the other wind directions – 43%. The lowest value of $< \text{AOT}(500) >$, 0.115 ± 0.217, was observed for westerly winds (225°–315°). This may be explained by the higher advection of clean air over Gotland: maritime Polar air was dominant during the summers of 1999–2003 (65%).

- A weak increase in the mean aerosol optical thickness with increasing relative humidity was found for northerly winds in all seasons and also for easterly winds in autumn (Figures 8a, 8b). An increase in mean $\alpha(440, 870)$ with RH was found for the N and W wind sectors in spring, the N, E and S sectors in summer, as well as the N and E sectors in autumn. In other cases, no impact of relative humidity on the Ångström exponent and AOT(500) was observed. It should be noted that the data presented here show the properties of aerosols occurring at various air humidities rather than the results of the hygroscopic growth of aerosols of a certain type. Aerosol load and composition at various humidities may vary.

- This analysis revealed the dependence of aerosol optical parameters (i.e. AOT(500) and $\alpha(440, 870)$) on meteorological factors, particularly on the wind direction and on relative humidity in each season. However, on the basis of the available dataset we were unable to draw any conclusions about the influence of wind speed, probably because the number of observations for high wind speeds was too low or because many factors simultaneously affect the variability in AOT(500) and $\alpha(440, 870)$.

Acknowledgements

References

Birmilli W., Wiedensohler A., Heintzenberg J., Lehmann K., 2001, *Atmospheric particle number size distribution in central Europe: statistical relations to air masses and meteorology*, J. Geophys. Res., 106 (D23), 32 005–32 018.

Carlund T., Hakånsson B., Land P., 2005, *Aerosol optical depth over the Baltic Sea derived from AERONET and SeaWiFS measurement*, Int. J. Remote Sens., 26 (2), 233–245.

Chylek P., Henderson B., Mishchenko M., 2003, *Aerosol radiative forcing and the accuracy of satellite aerosol optical depth retrieval*, J. Geophys. Res., 108 (D24), 4764 pp.

d'Almeida G., Koepke P., Shettle E. P., 1991, *Atmospheric aerosols: global climatology and radiative characteristics*, A. Deepak Publ., Hampton, Va., 561 pp.

Draxler R. R., Rolph G. D., 2003, *HYSPLIT (HYbrid Single-Particle Lagrangian Integrated Trajectory) Model access via NOAA ARL READY Website*, http: //www.arl.noaa.gov/ready/hysplit4.html, NOAA Air Resour. Lab., Silver Spring, MD.

Dubovik O., Holben B., Eck T. F., Smirnov A., Kaufman Y. J., King M. D., Tanré D., Slutsker I., 2002, *Variability of absorption and optical properties of key aerosol types observed in worldwide locations*, J. Atmos. Sci., 59 (3), 590–608.

Dubovik O., King M. D., 2000, *A flexible inversion algorithm for retrieval of aerosol optical properties from Sun and sky radiance measurements*, J. Geophys. Res., 105 (D16), 20 673–20 696.

Eck T. F., Holben B. N., Reid J. S., Dubovik O., Smirnov A., O'Neill N. T., Slutsker I., Kinne S., 1999, *Wavelength dependence of the optical depth of biomass burning, urban, and desert dust aerosols*, J. Geophys. Res., 104 (D24), 31 333 –31 350.

El-Metwally M., Alfaro S. C., Abdel Wahab M., Chatenet B., 2008, *Aerosol characteristics over urban Cairo: seasonal variations as retrieved from Sun photometer measurements*, J. Geophys. Res., 113, D14219, doi:10.1029/2008JD009834.

Formenti P., Andreae M. O., Andreae T. W., Galani E., Vasaras A., Zerofos C., Amiridis V., Orlovsky L., Karnieli A., Wendisch M., Wex H., Holben B. N., Maenhaut W., Lelieveld J., 2001, *Aerosol optical properties and large-scale transport of air masses: observation at a coastal and a semiarid site in the eastern Mediterranean during summer 1998*, J. Geophys. Res., 106 (D9), 9807 –9826.

Gao B.-C., Montes M. J., Ahmad Z., Davis C. O., 2000, *Atmospheric correction algorithm for hyperspectral remote sensing of ocean color from space*, Appl. Optics, 39 (6), 887–896.

Glantz P., Nilsson D. E., von Hoyningen-Huene W., 2006, *Estimating a relationship between aerosol optical thickness and surface wind speed over the ocean*, Atmos. Chem. Phys. Discuss., 6, 11 621–11 651.

Holben B. N., Eck T. F., Slutsker I., Tanre D., Buis J. P., Setzer A., Vermote E., Reagan J. A., Kaufman Y. J., Nakajima T., Lavenu F., Jankowiak I., Smirnov A., 1998, *AERONET – a federated instrument network and data archive for aerosol characterization*, Remote Sens. Environ., 66 (1), 1–16.

Holton J. R., Curry J. A., Pyle J. A., 2003, *Encyclopaedia of atmospheric science*, Vol. 1, Acad. Press, Amsterdam, Boston, 53 pp.

Ichoku C., Kaufman Y. J., Remer L. A., Levy R., 2004, *Global aerosol remote sensing from MODIS*, Adv. Space Res., 34, 820–827.

Jeong M.-J, Li Z., Andrews E., Tsay S.-C., 2007, *Effect of aerosol humidification on the column aerosol optical thickness over the Atmospheric Radiation Measurement Southern Great Plains site*, J. Geophys. Res., 112, D10202, doi:10.1029/2006JD007176.

Kastendeuch P. P., Najjar G., 2003, *Upper-air wind profiles investigation for tropospheric circulation study*, Theor. Appl. Climatol., 75, 149–165.

Kauffman Y. J., Smirnov A., Holben B. N., Dubovik O., 2001, *Baseline maritime aerosol: methodology to derive the optical thickness and scattering properties*, Geophys. Res. Lett., 28 (17), 3251–3254.

Kratzer S., Vinterhav C., 2010, *Improvement of MERIS level 2 products in Baltic Sea coastal areas by applying the Improved Contrast between Ocean and Land processor (ICOL) – data analysis and validation*, Oceanologia, 52 (2), 211–236.

Kuśmierczyk-Michulec J., 2009, *Ångström coefficient as an indicator of the atmospheric aerosol type for a well-mixed atmospheric boundary layer: Part 1: Model development*, Oceanologia, 51 (1), 5–38.

Kuśmierczyk-Michulec J., de Leeuw G., Gonzalez C. R., 2002, *Empirical relationships between mass concentration and Ångström parameter*, Geophys. Res. Lett., 29 (7), 1145, doi:10.1029/2001GL014128.

Kuśmierczyk-Michulec J., Marks R., 2000, *The influence of sea-salt aerosols on the atmospheric extinction over the Baltic and North Seas*, J. Aerosol Sci., 31 (11), 1299–1316.

Kuśmierczyk-Michulec J., Rozwadowska A., 1999, *Seasonal changes of the aerosol optical thickness for the atmosphere over the Baltic Sea – preliminary results*, Oceanologia, 41 (2), 127–145.

Kuśmierczyk-Michulec J., Schulz M., Ruellan S., Krüger O., Plate E., Marks R., de Leeuw G., Cachier H., 2001, *Aerosol composition and related optical properties in the marine boundary layer over the over the Baltic Sea*, J. Aerosol Sci., 32 (8), 933–955.

Niemi J. V., Tervahattu H., Koskentalo T., Sillanpää M., Hillamo R., Kumala M., Vehkamäki H., 2003, *Studies on the long-range transport episodes of particles in Finland in March and August 2002*, No. 10, Helsinki Metropolit. Area Council, Helsinki, 58 pp.

Niemi J. V., Tervahattu H., Vehkamäki H., Martikainen J., Laakso L., Kumala M., Aarnio P., Koskentalo T., Sillanpää M., Makkonen U., 2005, *Characterization of aerosol particles episodes in Finland caused by wildfires in Eastern Europe*, Atmos. Chem. Phys., 5 (8), 2299–2310.

O'Neill N. T., Eck T. F., Holben B. N., Smirnov A., Dubovik O., Royer A., 2001, *Bimodal size distribution influence on the variation of Angstrom derivatives in spectral and optical depth space*, J. Geophys. Res., 106 (D9), 9787–9806.

Pan W., Tatang M. A., McRae G. J., Prinn R. G., 1997, *Uncertainty analysis of direct radiative forcing by anthropogenic sulfate aerosols*, J. Geophys. Res., 102 (D18), 21 915–21 924.

Petelski T., 2003, *Marine aerosol fluxes over open sea calculated from vertical concentration gradients*, J. Aerosol Sci., 34 (3), 359–371.

Pugatshova A., Reinart A., Tumm E., 2007, *Features of the multimodal aerosol size distribution depending on the air mass origin in the Baltic region*, Atmos. Environ., 41 (21), 4408–4422.

Rapti A. S., 2005, *Spectral optical atmospheric thickness dependence on the specific humidity in the presence of continental and marine air masses*, Atmos. Res., 78 (1–2), 13–32.

Reiff J., Forbes G. S., Spieksma F., Reynders J. J., 1986, *African dust reaching Northwestern Europe: a case study to verify trajectory calculation*, J. Clim. Appl. Meteorol., 25 (1), 1543–1567.

Rolph G. D., 2003, *Real-time Environmental Applications and Display sYstem (READY) Website*, http://www.arl.noaa.gov/ready/hysplit4.html), NOAA Air Resour. Lab., Silver Spring, MD.

Ruddick K. G., Ovidio F., Rijkeboer M., 2000, *Atmospheric correction of SeaWiFS imagery for turbid coastal and inland waters*, Appl. Optics, 39 (6), 897–912.

Satheesh S. K., Moorthy K. K., 2005, *Radiative effects of natural aerosols: a review*, Atmos. Environ., 39 (11), 2089–2110.

Schroeder Th., Behnert I., Schaale M., Fischer J., Doerffer R., 2007, *Atmospheric correction algorithm for MERIS above case-2 waters*, Int. J. Remote Sens., 28 (7), 1469–1486.

Seinfeld J. H., Pandis S. N., 1998, *Atmospheric chemistry and physics: from air pollution to climate change*, Wiley, New York, 1326 pp.

Smirnov A., Holben B. N., Eck T. F., Dubovik O., Slutsker I., 2000, *Cloud-screening and quality control algorithms for the AERONET database*, Remote Sens. Environ., 73 (3), 337–349.

Smirnov A., Holben B. N., Eck T. F., Dubovik O., Slutsker I., 2003, *Effect of wind speed on columnar aerosol optical properties at Midway Island*, J. Geophys. Res., 108 (D24), 10 4802 pp.

Smirnov A., Royer A., O'Neill N. T., Tarussov A., 1994, *A study of link between synoptic air mass type and atmospheric optical parameters*, J. Geophys. Res., 99 (D10), 20 967–20 982.

Smirnov A., Villevalde Y., O'Neill N. T., Royer A., Tarussov A., 1995, *Aerosol optical depth over the ocean: analysis in term of synoptic air mass type*, J. Geophys. Res., 100 (D8), 16 639–16 650.

Stigebrandt A., Gustafsson B. G., 2003, *Response of the Baltic Sea to climate change-theory and observations*, J. Sea Res., 49 (4), 243–256.

Swietlicki E., Zhou J., Berg O. H., Martinsson B. G., Frank G., Cederfelt S.-I., Dusek U., Berner A., Birmilli W., Wiedensohler A., Yuskiewicz B., Bower K. N., 1999, *A closure study of sub-micrometer aerosol particle hygroscopic behaviour*, Atmos. Res., 50 (3–4), 205–240.

Tang I. N., 1996, *Chemical and size effects of hygroscopic aerosols on light scattering coefficient*, J. Geophys. Res., 101 (D14), 19 245–19 250.

Terpugova S. A., Panchenko M. V., Kozlov V. S., Polkin V. V., Yausheva E. P., 2004, *The study of the growth factor of the aerosol scattering coefficient in the near-ground layer of the atmosphere in West Siberia*, European Aerosol Conference, Budapest.

Weller M., Leiterer U., 1998, *Experimental data on spectral aerosol optical thickness and its global distribution*, Beitr. Phys. Atmos., 61 (1), 1–9.

Zieliński T., 2006, *Fizyczne właściwości przywodnej warstwy aerozolu w brzegowym obszarze morza*, Rozpr. Monogr. 18, IO PAN, Sopot, 164 pp.